GEOPHYSICAL RESEARCH LETTERS, VOL. 33, L24405, doi:10.1029/2006GL028282, 2006

Click Here for Full Article

Combined time-series resistivity and geochemical tracer techniques to examine submarine groundwater discharge at Dor Beach, Israel

P. W. Swarzenski,[1] W. C. Burnett,[2] W. J. Greenwood,[3] B. Herut,[4] R. Peterson,[2] N. Dimova,[2] Y. Shalem,[5] Y. Yechieli,[6] and Y. Weinstein[5]

Received 27 September 2006; revised 7 November 2006; accepted 13 November 2006; published 23 December 2006.

[1] A high-resolution, stationary geophysical and geochemical survey was conducted at Dor Beach, Israel, to examine the shallow coastal hydrogeology and its control on the exchange of submarine groundwater with the shallow Mediterranean Sea. Time-series resistivity profiles using a new 56 electrode (112-m long) marine cable produced detailed profiles of the fresh water/salt water interface and the subtle response of this interface to tidal excursions and other forcing factors. Such information, when ground-truthed with representative pore water salinities and formation resistivity values, can provide unique information of the extent and rates of submarine groundwater discharge (SGD). Time-series ^{222}Rn measurements of the adjacent coastal water column complemented these geophysical techniques and were modeled to yield integrated advective flow rates across the sediment/water interface, which at Dor Beach ranged from about 0 to 30 cm day^{-1} (mean = 7.1 cm d^{-1}), depending on the tidal range. Such results suggest that the underlying hydrogeologic framework at Dor is favorable for substantial SGD. Extrapolating these SGD estimates across a 100-m wide coastal zone implies that the Rn-derived SGD rate would equal ~7.1 m^3 d^{-1} per m of shoreline, and that the source of this discharging groundwater is a complex mixture of fresh groundwater derived from the upland Kurkar deposits, as well as locally recycled seawater.
Citation: Swarzenski, P. W., W. C. Burnett, W. J. Greenwood, B. Herut, R. Peterson, N. Dimova, Y. Shalem, Y. Yechieli, and Y. Weinstein (2006), Combined time-series resistivity and geochemical tracer techniques to examine submarine groundwater discharge at Dor Beach, Israel, *Geophys. Res. Lett.*, *33*, L24405, doi:10.1029/2006GL028282.

1. Introduction

[2] Dor Beach lies within the Carmel coastal plain about 25 km south of Haifa, Israel (Figure 1) and has been a site of vigorous archaeological research as evidence of past coastal civilizations has been traced back at least to ~3000 y before present [*Galili et al.*, 1988]. Along the Carmel coast evidence of dramatic sea-level change during the Late Holocene has been well documented [*Sivan et al.*, 2001]. For example, within our own study site, an old Arabic well that today is tidally inundated and thus defunct, was in 1915 located about 7.5 m from the coast line and still operational. This would imply that sea level at Dor Beach has risen more than 10 cm just this century [*Sneh and Klein*, 1984], and a 4 ky record suggests a maximum fluctuation of about ±1 m from present sea-level elevation (Figures 2a and 2b).

[3] In Dor, Holocene Nylotic sands cover Pleistocene N-S oriented sandstone ridges, known locally as 'kurkar' [*Sivan et al.*, 2001]. The Quaternary aquifer is underlain by the Carmel Cretaceous carbonate aquifer and although a direct hydraulic connection between these two aquifers has not directly been established at Dor Beach, the hydrogeologic control on coastal groundwater systems is well known. We examined the shallow coastal hydrogeology at Dor Beach using both time-series dc resistivity techniques as well as time-series ^{222}Rn. While Ra isotopes have been used to assess the marine or brackish contribution of submarine groundwater discharge into coastal waters [*Moore*, 1996, 2000; *Charette et al.*, 2001; *Swarzenski et al.*, 2006], as a noble gas produced by the decay of ^{226}Ra and recoil processes, ^{222}Rn will trace the total (fresh + recirculated) contribution of the discharged groundwater [*Burnett et al.*, 2003].

[4] The bi-directional exchange of coastal groundwater with sea water is an ubiquitous process driven by both marine and terrestrial processes [*Moore*, 2000; *Michael et al.*, 2005]. On the marine side, this exchange is complexly affected by water level fluctuations, i.e., waves, tides, and storms, as well as by density differences by the mixing of various water masses. Conversely, on the terrestrial side, Darcy's Law is made more complex by the underlying geologic framework and by the seasonality of hydrologic cycles that ultimately drive the flow of water seaward [*Taniguchi et al.*, 2002; *Michael et al.*, 2005]. While a globally averaged estimate of the volume of fresh groundwater exchanged across the sediment/water interface by these processes is at least an order of magnitude less than a similar estimate for river discharge [*Burnett et al.*, 2003], chemical transformations within coastal aquifers can render the SGD-derived constituent flux as an important, yet often unquantified, component of a coastal material mass balance [*Capone and Bautista*, 1985; *Charette et al.*, 2001; *Burnett et al.*, 2003].

2. Methods

2.1. Time Series Resistivity

[5] The use of electrical resistivity techniques to measure the conductivity (resistivity = electrical conductivity^{-1}) of

[1]U.S. Geological Survey, St. Petersburg, Florida, USA.
[2]Department of Oceanography, Florida State University, Tallahassee, Florida, USA.
[3]ETI, St. Petersburg, Florida, USA.
[4]Israel Oceanographic and Limnological Research, Haifa, Israel.
[5]Department of Geography and Environment, Bar-Ilan University, Ramat-Gan, Israel.
[6]Geological Survey of Israel, Jerusalem, Israel.

Copyright 2006 by the American Geophysical Union.
0094-8276/06/2006GL028282$05.00

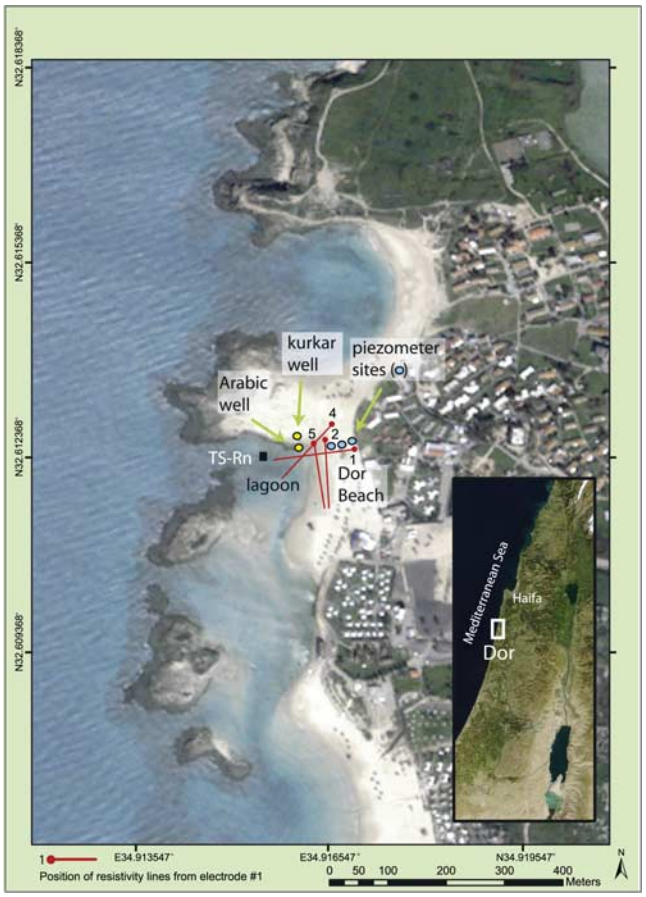

Figure 1. Study site, showing the time-series resistivity lines within Dor Beach, Israel. TS-Rn denotes location of the boat used for time-series ^{222}Rn measurements. The old Arabic well, the kurkar well, and three piezometer locations are also depicted.

coastal sediments and pore fluids has recently advanced considerably with the development of streaming and stationary marine cable configurations and multichannel systems [*Manheim et al.*, 2004; *Swarzenski et al.*, 2004, 2006]. Advantages of such systems over traditional horizontal dc methods that have been used with success to study the fresh water/salt water interface [*Hagemeyer and Stewart*, 1991] include rapid, multi-pole data acquisition across broad reaches of a land/sea margin. While several groups are currently using such marine systems in streaming mode to study coastal hydrogeologic processes, we used a new resistivity cable with 56 electrodes spaced 2-m apart in either shore-perpendicular (line1), shore-parallel (line2,5), or shore-diagonal (line4) configurations across Dor Beach and into the adjacent lagoon (Figure 1). Direct contact of the electrodes to the sediment was facilitated with wet sand bags or short metal spikes. This high resolution time-series resistivity system permits very detailed examination of the coastal hydrogeology and the response of the fresh water/salt water interface to tidal fluctuations to decimeter depths.

[6] At Dor, we surveyed the resistivity of the underlying sediments in March 2006 using an Advanced Geosciences Inc. (AGI) Marine SuperSting R8 multichannel system connected to an external switching box that controlled the flow of current along the 56-electrode cable. This system is programmed to measure current potentials in a distributed array so that resolution and signal-to-noise ratio is maximized. For a single resistivity measurement that takes on average just over 1 sec, the SuperSting R8 injects an optimized current, reverses the polarity and then injects the current again in order to cancel spontaneous voltages that may exist down cable. This process is cycled twice and if the error is less than a pre-determined threshold (i.e., 7%), then the next reading advances. Multiple replicates are programmed into the instrument to account for wave- and pore fluid-induced noise.

[7] The resistivity measurements were processed using an updated inverse modeling routine within AGI's EarthImager software that accommodates the water column salinity and depth. The processing resolution was optimized by using a starting model with the apparent resistivity pseudo-section coupled to real bathymetry and conductivity/temperature data collected at electrode 28 and 56. The best-fitting layered model was then developed using an iterative least

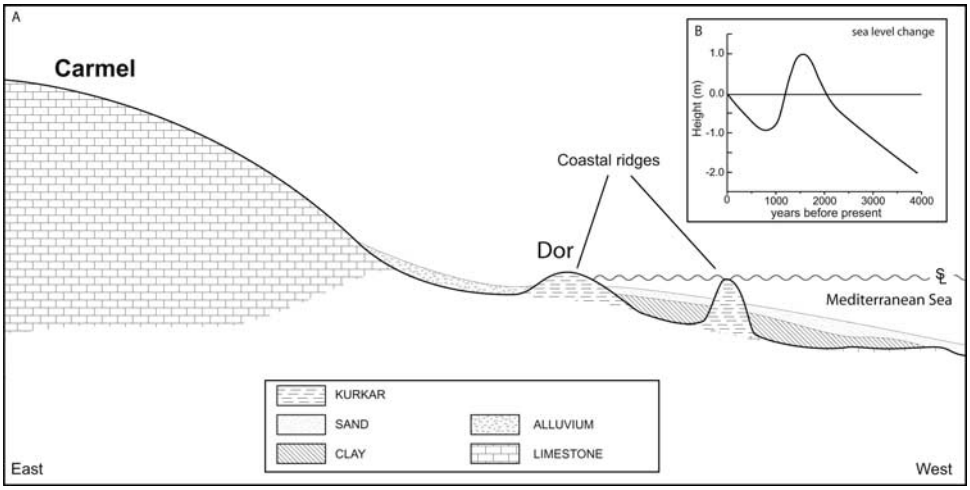

Figure 2. (a) Idealized geologic cross-section at Dor, Israel [after *Galili et al.*, 1988], and (b) reconstructed late Holocene sea level curve for Dor, Israel [after *Sneh and Klein*, 1984].

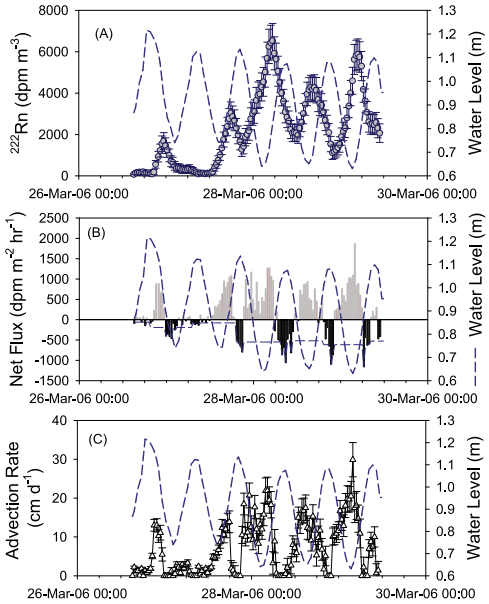

Figure 3. (a) ^{222}Rn (dpm L^{-1}), (b) net flux rates (dpm m^{-2} hr^{-1}), and (c) Rn-derived advection rates (cm d^{-1}) derived during a 4-day time series at Dor Beach. Averaged water levels shown as blue dashed line. A 12-hr mixing cycle and a 5-point moving average were used in the Rn calculations.

squares smooth model inversion method [*Greenwood et al.*, 2006].

2.2. Rn-222

[8] Rn-222 has been shown to be a particularly effective tracer of sediment/water interface exchange processes, including submarine groundwater discharge, in that this isotope is most often very enriched in groundwater relative to typical surface water, chemically inert, and radioactively decays at a rate ($t_{1/2}$ = 3.82 days) comparable to the time scales of many coastal processes [*Martens et al.*, 1980]. Recent advances in the analyses of Rn have been accomplished using a commercial Rn-in-air monitor and a simple water/air exchanger [*Burnett and Dulaiova*, 2003; *Dulaiova et al.*, 2005]. By knowing the temperature-dependent partitioning coefficient of Rn, one can calculate the Rn concentration in water from the measured air concentration. At Dor Beach, we measured the in situ, near-continuous ^{222}Rn concentration in the water column during a 4-day time series from a boat positioned at a site ~40m from shore using a submersible pump positioned at a fixed depth relative to the water line. Concurrent with the Rn analyses, a continuous record of the temperature, salinity, and depth of the water column was collected using a calibrated YSI multi-parameter probe and a HOBO Water Level recorder, respectively.

3. Results and Discussion

[9] To constrain the salinity regime of the coastal groundwater per se at Dor Beach, salinity and water levels were also measured in May 2006 in various piezometers and a kurkar well (Figure 1). The mean salinity within the 6-m deep coastal kurkar well was 3.7 ± 0.2 (n = 10) while groundwater levels varied directly with the tides. A piezometer located about 60 m from the high tide line had a mean salinity of 0.7 to 0.8, and a piezometer positioned closest to the high tide line exhibited a narrow range in mid salinity values (13–15). In contrast, salinities in the now defunct Arabic well ranged widely from 4.7 to 37.8, showing tidally-controlled seawater contamination.

[10] While submarine groundwater discharge (SGD) has been now recognized as an important potential vector for constituent transport to the coastal ocean [cf. *Burnett et al.*, 2003], only recent advances in both geochemical and geophysical techniques have made the identification and quantification of SGD into a coastal water body a realistic endeavor [*Moore*, 2000; *Burnett et al.*, 2003; *Manheim et al.*, 2004; *Swarzenski et al.*, 2006]. To examine the total (fresh + recirculated) submarine groundwater discharge flux rate into the coastal waters at Dor, we used ^{222}Rn as a natural tracer. Groundwater Rn-222 concentrations in the kurkar well at Dor were several orders of magnitude greater (mean ^{222}Rn = 350 ± 75 dpm L^{-1}) than those measured in the adjacent coastal waters (mean ^{222}Rn = 2.2 ± 1.8 dpm L^{-1}). Additional groundwater ^{222}Rn concentrations measured in several piezometers (^{222}Rn = 19 – 50 dpm L^{-1}) oriented shore-perpendicular across Dor Beach, the old Arabic well (mean ^{222}Rn = 320 ± 27 dpm L^{-1}) located just below the high tide line, and from two seepage meter samples (mean ^{222}Rn = 150 ± 29 dpm L^{-1}) placed within the lagoon, all ranged consistently between these two end member ^{222}Rn concentrations. From this range in groundwater ^{222}Rn concentrations, we used a mean value of 200 dpm L^{-1} to best represent the discharging submarine waters that were mixtures of fresh and saline groundwaters. For the 4-day time series, the water column ^{222}Rn concentrations (Figure 3a) ranged 0.1 to 6.53 dpm L^{-1}, with a mean of 2.2 ± 1.8 dpm L^{-1}.

[11] A mass balance for input and loss terms for coastal Rn can be established, as per methods of *Burnett and Dulaiova* [2003], to estimate an advection term. From such a model, a calculated net flux rate ranged from −370 ± 310 to 510 ± 390 dpm m^{-2} hr^{-1} (Figure 3b), and a mean water column mixing loss term of −410 ± 250 dpm m^{-2} hr^{-1} yielded advective flux rates (Figure 3c) that ranged from ~0 – 30 cm d^{-1}, with a mean of 7.1 ± 6.9 cm d^{-1} (n = 136). If we assume that most groundwater will discharge within a 100-m zone closest to shore, then the mean Rn-derived SGD rate would equal roughly 7.1 m^3 d^{-1} per m of shoreline. The observed range in groundwater ^{222}Rn concentrations at Dor confirms that the source of this discharging groundwater includes a complex mixture of fresh groundwater derived from the upland Kurkar deposits as well as locally recycled seawater. Seabed resistivity may identify sites or regions of submarine groundwater discharge and may also provide information on the salinity of these discharging fluids.

[12] Observed subsurface resistivity values (ohm-m) are a function of the underlying lithology, porosity, pore water salinity, and temperature. In saturated sediments these observed formation resistivities (R_f) reflect an integrated signal derived from both the resistivity of the sediment grains (R_s) and pore water resistivity (R_p). The resistivity of

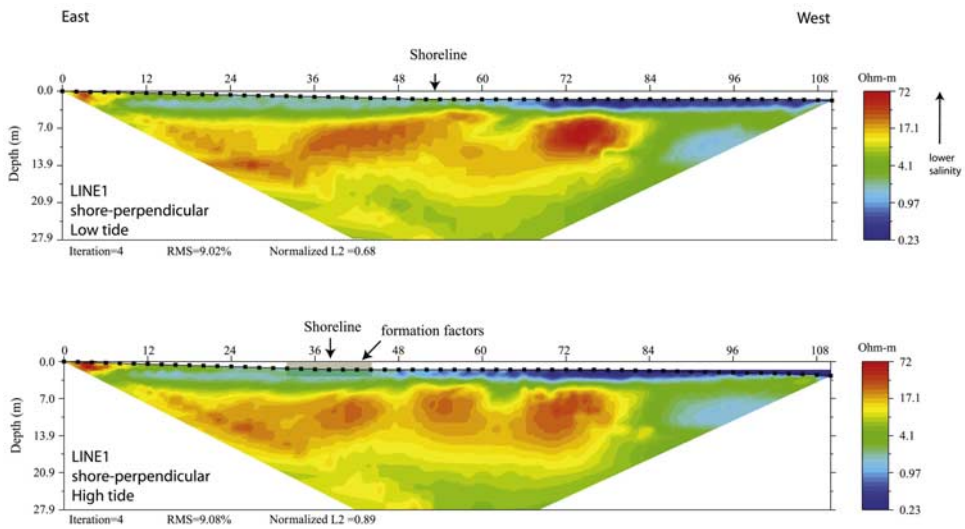

Figure 4. The inverted resistivity (ohm-m) distribution along a shore-perpendicular transect (line1) across Dor Beach looking south, during a 24-cm tidal range. Discussion on the conversion of formation resistivity (R_s) to formation factors, F, is centered on the shoreface, as identified by the gray box on the high tide image.

pore water (ohm-m) is easily defined by measuring the pore water salinity, S ($S = 7.042 * R_p^{-1.0233}$) [*Manheim et al.*, 2004]. The formation resistivity in representative lithologies can be manually measured using either a Wenner-type probe on discrete samples, or by measuring the direct resistance of saturated sediment between two electrodes. In saturated sediments, R_f values can be used to infer the formation factor, F, from the expression $F = R_f R_p^{-1}$. Assuming locally homogenous deposits, the formation factor, F, can then be used to interpret formation salinities from the time-series resistivity observations. At Dor Beach, we measured R_f in both the surficial sands as well as the adjacent underwater kurkar deposits. The sand R_f measurements were conducted close to the water line, which allowed us to assume that sediments were fully saturated (mean pore water salinity was 37.2 ± 3.8; n = 128). At these sites a mean R_f value for Dor Beach saturated sand was 1.85 ± 0.23 ohm-m. A similarly calculated mean R_f value of the kurkar rock on the distal (last 10m) end of the cable ranged up to 3.57 ± 2.17 ohm-m. Such R_f and R_p values yield formation factors that in Dor ranged from 8 to above 14 (mean = 9.4 ± 1.2; n = 85). These results are consistent with the notion that formation factors must increase as sediments become more consolidated and lithified [*Manheim et al.*, 2004].

[13] An advantage in interpreting resistivity values under stationary mode rather than streaming mode is that as the cable position does not change during data acquisition, observed fluctuations in resistivity can be attributed to dominant forcing factors alone, such as tidally-driven water level variations. The orientation and start of each line (electrode No. 1) is graphically depicted in Figure 1. The inverted resistivity (in ohm-m) distribution from a shore-perpendicular (line1) transect during a 24-cm tidal excursion at Dor Beach is shown in Figure 4. The mid-point of the 112-m cable was positioned close to the low tide line while roughly two thirds of the cable was submerged at high tide. From both low and high tide images, it is evident that a ~10-m thick, more resistive (i.e., fresher) layer extends seaward about 80m. Above this layer, seawater saturated surface sediments respond most dramatically to the tidal variations. While the observed tidal amplitude (24-cm) did not appear to significantly influence the overall resistivity regime, there are notable differences that do suggest preferential flushing of the sediments. Much of line1 traverses surficial beach sand deposits except towards the most seaward extent of the cable where sands are replaced by kurkar-type sandstone. It is notable that the resistivity regime in this segment of the line did not change with the tides, which would agree with the much lower hydraulic conductivities of bedrock relative to beach sand.

[14] An examination of the two shore-parallel lines (line2 and line5), where line5 was positioned closest to the high-tide line and line2 was located ~5-m upland, show similar patterns in the inverted resistivity (Figure 5). Both images collected at low tide show relatively lower resistivity (i.e., higher salinity) values close to the sediment/water interface and higher resistivities at the northern extent of the two lines and also with depth. A sharp contact of lower resistivity values was evident in the surface sediments to depths that ranged from ~3m to ~10m along the 112m cable. This suggests that much fresher groundwater lies beneath this less resistive layer and there is no evidence that this layer becomes much more saline at depths within the exploration depth. Considering that the two shore parallel lines transect line1 at different relative positions, the corresponding resistivity patterns agree well with those observed in line1.

[15] Figure 6 shows the inverted resistivity distribution along line4, which diagonally traverses the beach about 60-m (high tide) to 70-m (low tide) before ending on the submerged kurkar deposits of the central lagoon. The tidal range separating the two resistivity images was 45-cm. At low tide, persistent groundwater seepage (salinity = 4.4) was observed in the sands adjacent to the kurkar deposits and just above the water's edge. These observations were corroborated in the low-tide resistivity image; at 60 m to 62 m, a tongue of much fresher water extended upward to the surface sediments. If we assume that the discharging seepage waters (Figure 6; cell A) have a R_f value of

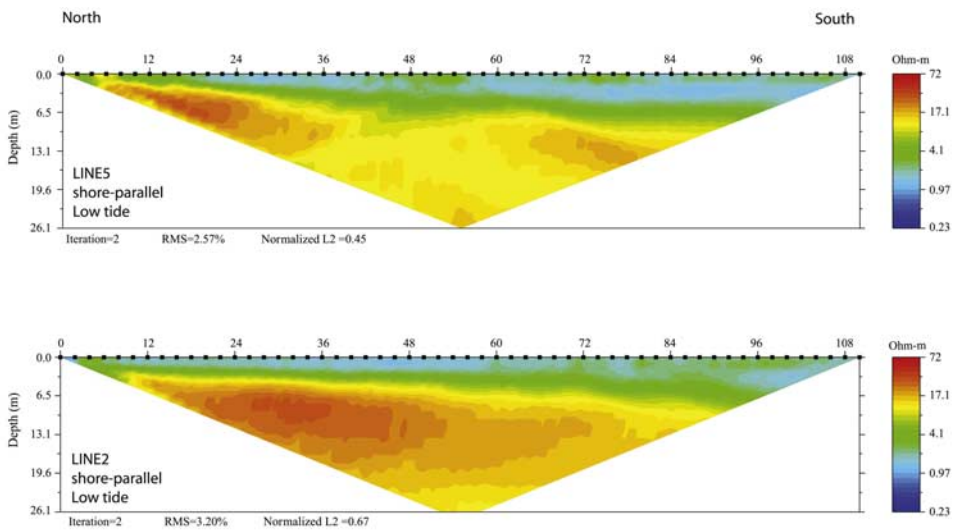

Figure 5. Inverted resistivity along two shore-parallel lines at Dor Beach. Line2 was positioned ~5m further landward from line5, which was placed along the low-tide water line.

~20 ohm-m based on the low tide measurements, then a mean formation factor of 9.4 generated for saturated sands would correspond to a salinity of about 3.3 – a value that is in close agreement to the observed salinity of the groundwater seeping out of the sands. Beyond ~78 m, the sharp contacts that separate the more resistive from the saline units appears virtually indistinguishable, while at 84 m, enhanced salt water intrusion or mixing at high tide was observed. A comparison of R_f values within cells A (see above) and B (R_f ~2 ohm-m; S = 34.4) yields a first-order, maximum groundwater exchange rate of about 7 m^3 d^{-1} per linear m (3m × 3m × 1m × 2 tidal cycles per d × porosity, 0.4), a value serendipitously close to the observed mean Rn-derived advection rate. While the Rn-derived SGD rate reflects an integrated estimate of fresh and/or salty water masses, the dc resistivity results yield detailed information of the specific location and salinity regime of the discharging fluids. Agreement in these two estimates suggests that near-shore exchange processes may dominate the SGD signal observed in the lagoon.

4. Conclusions

[16] High resolution time-series resistivity measurements at Dor Beach provided unique information on the coastal hydrogeologic framework that ultimately controls the exchange of submarine groundwater with the shallow Mediterranean Sea. Because the 56-electrode resistivity cable remains stationary on the seafloor during tidal

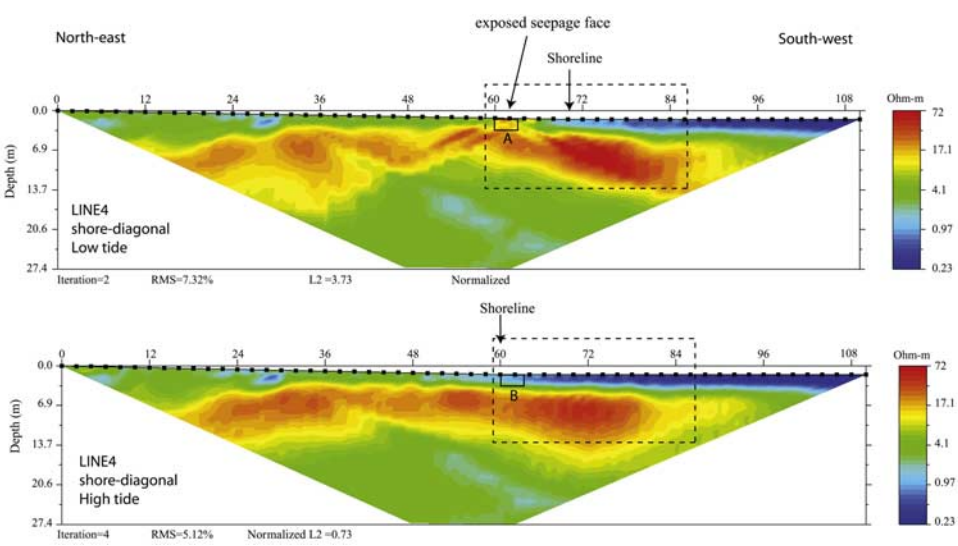

Figure 6. Inverted resistivity during low and high tide at line4, a shore-diagonal transect. Tidal range was 45-cm. Discussion in text is centered on the two dashed inset boxes that describe resistivity variations across the land/sea interface. Observed seepage just above the shoreline during low tide had a salinity of 4.4. First-order groundwater exchange rates from the resistivity data are assessed from the two identified cells: A (mean ~20 ohm-m; S = 3.3) and B (mean ~2 ohm-m; S = 34.4) using a formation factor, F, of 9.4.

excursions, one can in detail assess the impact of water level variations alone on the subsurface hydrogeology and fluid exchange processes across the sediment/water interface. By comparing inverted resistivity values within a cell from a shore-diagonal transect during low and high tides, we estimate a maximum, first-order groundwater exchange rate of about 7 m^3 d^{-1} per meter of shoreline. A coincident time-series ^{222}Rn study in the adjacent coastal waters yielded similar submarine groundwater discharge rates (mean = 7.1 cm d^{-1}; 7.1 m^3 d^{-1} per shoreline meter) that varied depending on the tides. Simultaneous geochemical tracer studies and high-resolution resistivity measurements demonstrate the complementary utility of these two techniques to study coastal exchange processes.

[17] **Acknowledgments.** This project was funded through a BiNSF grant 2002381. PWS specially thanks the USGS Coastal and Marine Geology Program for continued support in this field and Frank Manheim for enthusiastically exploring the utility of multichannel electrical resistivity as a novel tool in coastal hydrogeology. WCB acknowledges support from the National Science Foundation (OCE05-20723). Constructive reviews by Richard Poore (USGS), Sarah Kruse (USF) and two autonomous reviews greatly improved this manuscript. The use of trade names is for descriptive purposes only and does not imply endorsement by the U.S. Government.

References

Burnett, W. C., and H. Dulaiova (2003), Estimating the dynamics of groundwater input into the coastal zone via continuous radon-222 measurements, *J. Environ. Radioact.*, *69*, 21–35.

Burnett, W. C., H. Bokuniewicz, M. Huettel, W. S. Moore, and M. Taniguchi (2003), Groundwater and porewater inputs to the coastal zone, *Biogeochemistry*, *66*, 3–33.

Capone, D. G., and M. F. Bautista (1985), A groundwater source of nitrate in nearshore marine sediments, *Nature*, *313*, 214–216.

Charette, M. A., K. O. Buesseler, and J. E. Andrews (2001), Utility of radium isotopes for evaluating the input and transport of groundwater-derived nitrogen to a Cape Cod estuary, *Limnol. Oceanogr.*, *46*, 465–470.

Dulaiova, H., R. Peterson, and W. C. Burnett (2005), A multi-detector continuous monitor for assessment of ^{222}Rn in the coastal ocean, *J. Radioanal. Nucl. Chem.*, *263*, 361–365.

Galili, E., M. Weinstein-Evron, and A. Ronen (1988), Holocene sea-level changes based on submerged archaeological sites off the northern Carmel coast in Israel, *Quat. Res.*, *29*, 36–42.

Greenwood, W. J., S. Kruse, and P. W. Swarzenski (2006), Extending electromagnetic methods to map coastal pore-water salinities, *Ground Water*, *44*, 292–299.

Hagemeyer, R. T., and M. T. Stewart (1991), Resistivity investigations of salt-water intrusion near a major sea-level canal, in *Investigations in Geophysics* 5, edited by S. H. Ward, pp. 67–77, Soc. of Explor. Geophys., Tulsa, Okla.

Manheim, F. T., D. E. Krantz, and J. F. Bratton (2004), Studying ground water under DELMARVA coastal bays using electrical resistivity, *Ground Water*, *42*, 1052–1068.

Martens, C. S., G. W. Kipphut, and J. V. Klump (1980), Sediment-water chemical exchange in the coastal zone traced by in situ ^{222}Rn flux measurements, *Science*, *208*, 285–288.

Michael, H. A., A. E. Mulligan, and C. F. Harvey (2005), Seasonal oscillations in water exchange between aquifers and the coastal ocean, *Nature*, *436*, 1145–1148.

Moore, W. S. (1996), Large groundwater inputs to coastal waters revealed by ^{226}Ra enrichments, *Nature*, *380*, 612–614.

Moore, W. S. (2000), Determining coastal mixing rates using radium isotopes, *Cont. Shelf Res.*, *20*, 1995–2007.

Sivan, D., S. Wdowinski, K. Lambeck, E. Galili, and A. Raban (2001), Holocene sea level changes along the Mediterranean coast of Israel, based on archaeological observations and numerical model, *Palaeogeogr. Palaeoclimatol. Palaeoecol.*, *167*, 101–117.

Sneh, Y., and M. Klein (1984), Holocene sea level changes at the coast Dor, southeastern Mediterranean Sea, *Science*, *226*, 831–832.

Swarzenski, P. W., W. C. Burnett, C. Reich, H. Dulaiova, R. Martin, and J. Meunier (2004), Novel geophysical and geochemical techniques to study submarine groundwater discharge in Biscayne Bay, Florida, *U.S. Geol. Surv. Open File Rep.*, *2004-3117*.

Swarzenski, P. W., W. G. Orem, B. F. McPherson, M. Baskaran, and Y. Wan (2006), Biogeochemical transport in the Loxahatchee river estuary: The role of submarine groundwater discharge, *Mar. Chem.*, *101*, 248–265.

Taniguchi, M., W. C. Burnett, J. E. Cable, and J. V. Turner (2002), Investigations of submarine groundwater discharge, *Hydrol. Processes*, *16*, 2115–2129.

W. C. Burnett, N. Dimova, and R. Peterson, Department of Oceanography, Florida State University, Tallahassee, FL 32306, USA.

W. J. Greenwood, ETI, St. Petersburg, FL 33701, USA.

B. Herut, Israel Oceanographic and Limnological Research, Haifa, 31080, Israel.

Y. Shalem and Y. Weinstein, Department of Geography and Environment, Bar-Ilan University, Ramat-Gan, 52900, Israel.

P. W. Swarzenski, U.S. Geological Survey, St. Petersburg, FL 33701, USA. (pswarzen@usgs.gov)

Y. Yechieli, Geological Survey of Israel, Jerusalem, 95501, Israel.